



**HAL**  
open science

## **Power source evaluation of a wireless power transfer system**

Guillaume Vigneau, Mohamed Cheikh, R Benbouhout, Said Bouguer, Alexandru Takacs

► **To cite this version:**

Guillaume Vigneau, Mohamed Cheikh, R Benbouhout, Said Bouguer, Alexandru Takacs. Power source evaluation of a wireless power transfer system. IEEE Wireless Power Transfer Conference, May 2014, Jeju, South Korea. 4p., <10.1109/WPT.2014.6839615>. <hal-02066244>

**HAL Id: hal-02066244**

**<https://laas.hal.science/hal-02066244v1>**

Submitted on 13 Mar 2019

HAL is a multi-disciplinary open access archive for the deposit and dissemination of scientific research documents, whether they are published or not. The documents may come from teaching and research institutions in France or abroad, or from public or private research centers.

L'archive ouverte pluridisciplinaire HAL, est destinée au dépôt et à la diffusion de documents scientifiques de niveau recherche, publiés ou non, émanant des établissements d'enseignement et de recherche français ou étrangers, des laboratoires publics ou privés.



HAL Authorization

# Power Source Evaluation of a Wireless Power Transfer System

Guillaume Vigneau<sup>1,2,3</sup>, Mohamed Cheikh<sup>1</sup>, Rachid Benbouhout<sup>1</sup>, Said Bouguern<sup>1</sup>

<sup>1</sup> Continental Automotive SAS France  
Toulouse, France

<sup>1</sup> firstname.lastname@continental-corporation.com

Alexandru Takacs<sup>2,3</sup>

<sup>2</sup> CNRS, LAAS, 7 avenue du colonel Roche, 31400  
Toulouse, France

<sup>3</sup> Université de Toulouse, UPS, LAAS, 31400  
Toulouse, France

**Abstract**—With more than 230 products on store shelves and an estimation of 100 million wireless power devices in use by 2015 (IHS source), the wireless power market is rapidly growing. Moreover, current smartphones are used with several applications (music streaming, satellite navigation system or even NFC virtual key for car sharing) and thus a convenient power supply system is required. This paper addresses the complete modeling and characterization of this power source in a Wireless Power Transfer context by an original modeling approach. A good correlation between measurement and simulation is obtained both for electrical (e.g. input impedance, power, etc.) and electromagnetic (e.g. magnetic field) quantities. Through simulations performed on commercial software's, the correlation simulation/measurement shows a difference of only 2% on the active power available on the load and the modeled behavior of the magnetic field corroborates with the measured one.

**Index Terms** — Wireless power transfer, inductive coupling, electromagnetic modeling, electronic circuit simulation, automotive systems, power budget

## I. INTRODUCTION

Today, there are more and more applications qualified of wireless. Wirelessly powering nomad objects (smart phones, cellular phone, personal computer, GPS system, etc.) seems to be a very smart and ergonomic solution [1]. To implement a wireless powering system there are basically three approaches: reactive near-field coupling (inductive and resonant) [2]-[3], far-field directive power beaming [4] and far-field nondirective power transfer [5]. In order to guarantee the interoperability between wireless power devices designed by different manufacturers, organizations like the Wireless Power Consortium (WPC) [6], the Power Matter Alliance (PMA) [7] or the Alliance for Wireless Power (A4WP) [8] has been established. The Wireless Power Consortium made a low power standard (named “Qi”) for providing up to 5 Watts to a compliant receiver, with specific designs and recommendations [6]. A classical Wireless Power Transfer System (WPTS) is illustrated in Fig. 1. The power transfer between the transmitter (Tx) and the receiver (Rx) is made by using coupled coils separated by a distance ( $d$ ) and having a coupling factor ( $k$ ) [9]. For automotive applications, the power supply is the car’s battery whereas the load could be a nomadic electronic system. A possible application embedded in vehicle is illustrated in Fig. 2.

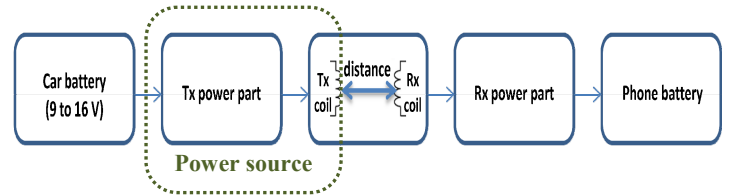


Fig. 1. Schema of a typical inductive WPTS



Fig. 2. Illustration of a WPTS in a vehicle environment

This paper proposes a new approach to model and to characterize our WPTS. It is crucial in a development phase of an industrial product to perform a realistic modeling of the WPTS. The simulation/theoretical models are intensively used along the design and the optimization process of such an industrial product (before the final prototyping). Consequently, the correlation between simulation and measurement is analyzed all over this study to corroborate the different results allowing us to validate and fine-tune our simulation model.

## II. ELECTROMAGNETIC MODELING AND CHARACTERIZATION OF THE TRANSCIEVER COILS

As shown in Fig. 1, the coupled coils are an important part of the WPTS. Two types of WPTS coils were designed and modeled using the commercial field solver FEKO (EM Software & Systems - S.A). The electrical and magnetic parameters were measured on prototyped samples and compared to the simulation results.

Most of WPTS uses two types of coil technologies, based on Litz wires [10] or on a Printed Circuit Board (PCB) [11]-[12]. Litz wires are a special type of cable used to carry alternating currents (consisting of multiple strands) and designed to significantly reduce the losses. Due to the reduction of proximity effects, Litz coils have usually a good quality factor

(around 100). The PCB coils are made by printing metallic strips with an appropriate shape directly on the PCB, and the major advantages are an easy fabrication process and a lower price compared to Litz coils. But the main drawbacks are the lower quality factor (around 15) and higher thermal dissipation than Litz technology. Litz and PCB Coils are respectively named as “A6” and “B5” in the Qi low power designs used here [13]. A magnetic permeable material (ferrite) positioned on the coils’ backs improves the quality and coupling (between two coils) factors. This ferrite is also used as shielding against the undesired magnetic field emitted behind the coils and protects the transmitter’s electronic circuitry of electromagnetic interferences.

#### A. Electromagnetic modeling and characterization techniques

The electromagnetic simulations were performed in FEKO by using the Method Of Moments (MoM) with Volume Equivalence Principle (VEP) and Low Frequency (LF) stabilization techniques on a twenty-nodes (CPU cores) cluster. Meshing is a critical point in all electromagnetic simulations, defining how precisely Maxwell’s equations are solved by using a finite elements discretization of the geometry. For example on the B5 design, the four PCB coils are totally meshed with 2590 triangles and 882 tetrahedrons for the ferrite (triangle and tetrahedron are respectively used to mesh metallic surfaces and dielectric volumes). The adopted mesh is a good trade-off between the accuracy and the simulation time. The four coils are implemented with copper strips and the ferrite (thickness: 2.2 mm) has a relative magnetic permeability of 800 and a magnetic loss tangent of 0.00008 (the same ferrite will be used all over this study).

The Litz wires of A6 coils were modeled as a unique copper wire of equivalent radius and the ferrite is the same than the one used for the B5 PCB coils.

To validate the electromagnetic modeling accuracy, the coils with ferrite on the back have been prototyped as shown on the Fig. 3. Their inductance (L) and Equivalent Series Resistance (ESR) are measured through an impedance analyzer. The magnetic field is measured with a H-field meter (Maschek 3D H/E field meter ESM-100) at different distances of the coils.

#### B. Electrical parameters of coils

The simulated and measured electrical parameters (inductance L and equivalent series resistance ESR) are presented for both Litz and PCB coils in the Table I. To compare the different results between modeling and experimentation, the electrical parameters are extracted at different frequencies (100, 150 and 200 kHz).

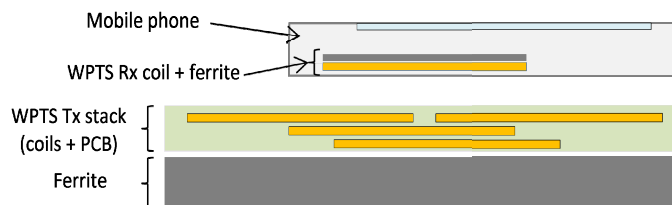


Fig. 3. Schematic of Tx coils assembly coupled with the Rx system

TABLE I  
ELECTRICAL PARAMETERS CORRELATION FOR A6 & B5 COILS

	Freq. (kHz)	ESR (mΩ)		L (μH)	
		Meas	FEKO	Meas	FEKO
A6 Design	100	85	97.25	11.17	11.98
	150	100	115.3		
	200	123	131.5		
B5 Design	100	339	503	8.43	8.75
	150	417	530	8.39	8.72
	200	507	553	8.36	8.71

We can observe a relative good correlation between simulated and measured results. Measured and simulated inductance values are very close over the chosen/operating frequencies. As expected, coils’ ESR is higher for PCB (B5) than Litz (A6) structures. However the correlation simulation/measurement of the ESR is better with PCB than Litz coils because Litz models have been simplified within FEKO through a unique copper wire instead of a several strands structure (105 strands). A correction factor of  $c = 1.801$  was established based on the analytical computation of the ohmic losses (they are predominant at such low frequencies) taking into account the realistic case (105 strands of radius  $r = 0.004$  mm) and the equivalent radius used by the simulation model (radius  $r = 0.55$  mm). The results depicted in Table I take into account the correction factor. With this correction, we obtain a good correlation between simulation and measurement for both A6 and B5 structures and for both ESR and inductance values. The small differences between simulation and experimental results can be explained by the accuracy issues of the adopted simulation model/approach at such low frequencies and for such a complex geometry.

#### C. Magnetic field of coils

A WPTS exploiting the near field inductive coupling uses the magnetic field to transfer energy from a coil to another. So a main step in the wireless power source study described in this paper is the magnetic field characterization and its compliance with reference exposure limits. This is a critical point due to the close proximity of persons inside the car. Independently of the region where the product will be implanted, basic restrictions on Electro-Magnetic Field (EMF) limits of ICNIRP [14] or IEEE C95.1.2005 [15] are applicable. For example, ICNIRP 2010 Guidelines recommend a reference level of 21 A/m for the magnetic field strength while IEEE advises a maximum permissible exposure of 163 A/m for head/torso and 900 A/m for limbs.

In this study the magnetic field is generated by a power source operating at 110 kHz with a current of 1 A rms injected into the coils (both for A6 and B5 designs), that is the typical current needed in a 5 Watts WPTS. Fig. 4 and Fig. 5 show the simulated (FEKO) and measured magnetic field at different distances for the B5 PCB and A6 Litz coils while the ferrite shielding impact on the magnetic field is depicted in Fig. 6. Supposing that the coil under test (A6 or B5) is positioned in the horizontal plane (e.g. “xy” plane), the distance is measured on a vertical axis (Oz) between the geometrical (symmetry) center of the coil and the measuring (or simulating) point. We note a good correlation between measurement and simulation and the curves follow

$$m = \frac{1}{N} \sum_{i=1}^N \frac{B(i) \cdot 4 \cdot \pi \cdot d(i)^3}{\mu_0 \cdot \sqrt{P}} \quad (1)$$

Where:

$m$  is the magnetic moment,  $N$  the number of samples (between the distance of  $d(1) = 0.5$  m to  $d(6) = 1$  m from coils with a step of 0.1 m),  $B(i)$  the magnetic field at  $i$ ,  $\mu_0$  the magnetic permeability and  $P$  the reactive power into the coil.

At long distances (over than 50 cm), the PCB coils generates slightly higher fields than A6 Litz. The estimated magnetic moments of B5 and A6 coils are respectively  $0.0148 \text{ A.m}^2/\sqrt{W}$  and  $0.0132 \text{ A.m}^2/\sqrt{W}$ .

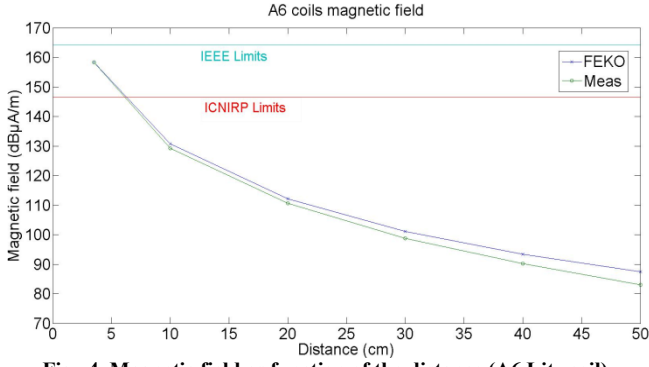


Fig. 4. Magnetic field as function of the distance (A6 Litz coil)

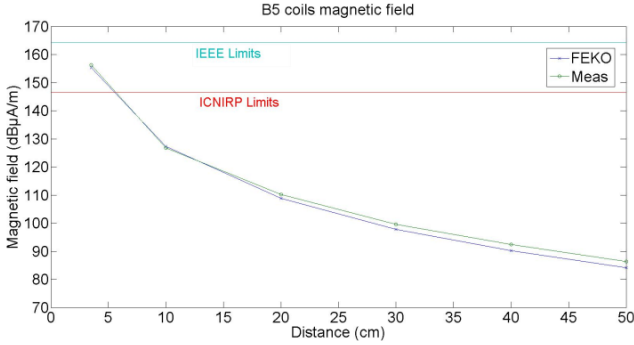


Fig. 5. Magnetic field as function of the distance (B5 PCB coil)

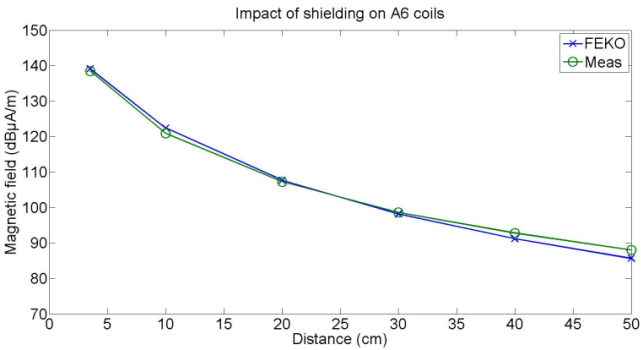


Fig. 6. Impact of the ferrite on the magnetic field (A6 Litz coil)

the same trend for each case. The correlation is lower for large distances ( $> 40$  cm) where the magnetic field is weak and subject to noise and field distortions leading to measurement uncertainties. Fig. 6 illustrates the ferrite impact on the magnetic field. Experimental and simulation curves show that the magnetic field is lower with  $20 \text{ dB}\mu\text{A/m}$  at 3 cm (A6 design) on the bottom side of the ferrite compared with the value measured on the top side of the Tx coil proving thus the shielding effect of the ferrite. The distance measured here (Fig. 6) is always on Oz axis but the measuring/simulation point is situated below the ferrite.

Concerning the EMF limits, Fig. 4 and Fig. 5 show that the radiated magnetic field is below the levels imposed by both IEEE and ICNIRP recommendations for the two coils (A6 and B5) for a distance greater than 7 cm.

Theoretical magnetic moments of the A6 (Litz wire) and B5 (PCB) models are estimated using the following formula:

### III. WPTS CIRCUIT SIMULATIONS AND CORRELATION WITH MEASUREMENTS

The electronic architecture of our power source has been designed, simulated and prototyped. It will be illustrated only with A6 Litz coils results because the same electronic architecture is used for B5 coils. The power source is coupled with a Qi compliant receiver, following the schematic presented in Fig. 1, for a delivered power of 5 Watts to the external load.

#### A. Modeling and measurement setup

The proposed modeling and simulation approach is based on the use of the commercial electronic circuit simulator Orcad PSPICE (Cadence Design System, Inc.) to model the complete WPTS (including transmitter and receiver circuitry). To provide a global simulation approach, the coils (Transmitter Tx and Receiver Rx) are defined as coupled coils characterized by their inductances  $L_p$  (primary: Tx coil) and  $L_s$  (secondary: Rx coil) and the coils' coupling factor ( $k$ ). The coupling factor ( $k$ ) is given by the following formula:

$$k = \frac{U_s}{U_p} \sqrt{\frac{L_p}{L_s}} \quad (2)$$

where  $U_p$  and  $U_s$  are respectively the voltages across the input ports of the primary (Tx) and secondary (Rx) coils while  $L_p$  and  $L_s$  are the Tx and Rx coils' inductances. Measured values are taken into account in (2).

The transmitter used (homemade product) is also compliant with the Qi A6 design. According to the Fig. 7, it consists of a DC-DC conversion stage (not represented here) connected to the DC-AC stage linked up to the resonant LC circuit through a low pass filtering formed by the inductance ( $L_f$ ) and the capacitance ( $C_f$ ).

The DC-AC conversion uses a class-D power amplifier realized by a half bridge inverter (2 transistors) which drives the primary coil ( $L_p$ , transferring the energy to the receiver's secondary coil) and the system is matched with the resonant capacitor ( $C_p$ ) in order to improve the power transfer.

Due to automotive applications, the energy supplying the power transmitter comes from the car's battery. A DC-DC conversion stage is included in order to regulate the DC power supplying the inverter and thus the amount of power transmitted to the receiver. SPICE models were used (transistors, diodes, etc.) and driving circuits were

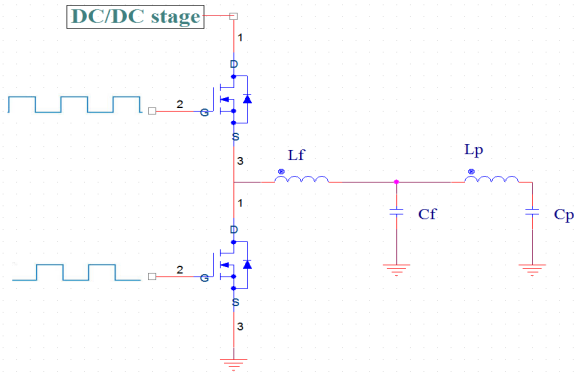


Fig. 7. Tx SPICE electronic circuit of the WPTS

implemented in order to make a complete transient study with specific logical driving signals. The primary Tx coil employed here has an inductance of  $L_p = 11.25 \mu\text{H}$  and an ESR of  $0.1 \Omega$  with a coupling factor  $k = 0.53$ . The receiver is compliant with the Qi TPR#5 architecture [13] and uses a Litz coil to receive power from the transmitter.

In the simulation setup, the components' values and coupling factor are implemented in the circuit. The following results are given with the Tx coil coupled to the Rx coil, for a transferred power of 5 Watts on the load.

#### B. Simulation and measurement results

First, the correlation between SPICE simulation (Tx model of the Fig. 7) and experimental results was investigated by analyzing the transient waveforms correctness (waveforms represented in Fig. 8). Secondly, the active power available across the transmitter coil is computed (average value over one period of the product between instantaneous voltage and current).

As shown in Fig. 8, a very good correlation for the simulated and measured waveform was obtained. The peak to peak measured voltage is 31.89 V (current: 4.41 A) while the peak to peak simulated voltage is 33.26 V (current: 4.41 A). The effective (rms) voltage, current and the power available on the Tx coil were extracted from the simulated and measured curves and are summarized on the Table II. A good correlation (close to 2%) between theoretical modeling and experimental measurement validates the proposed circuit simulation approach.

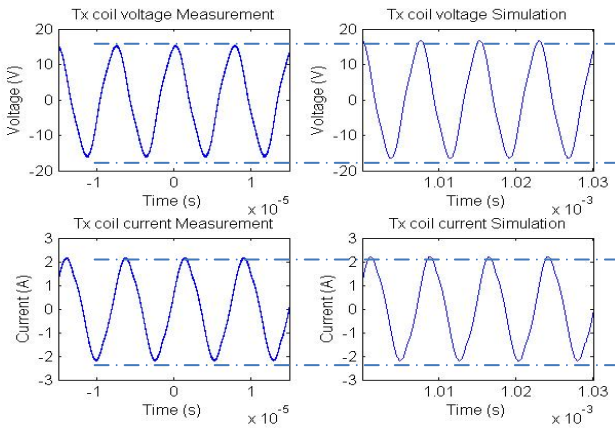


Fig. 8. Voltage and current waveforms (measured and simulated) on the Tx coil

TABLE II  
CORRELATION BETWEEN ELECTRONIC MEASUREMENTS AND SIMULATIONS

	Voltage ( $V_{\text{rms}}$ )	Current ( $A_{\text{rms}}$ )	Active power (W)
Measurement	10.61	1.46	6.57
Simulation	11.17	1.5	6.43
Correlation (%)	5.01	2.67	2.18

#### IV. CONCLUSION

This paper addresses the full characterization of a wireless power source, compliant with a Qi WPTS, from a simulation and measurement's point of view. Electromagnetic simulation models were used for the coils while circuit simulation was adopted for the driving electronic circuitry. Electrical parameters of modeled coils and the radiated magnetic field are well recovered by the measurements despite of the use of simplified electromagnetic models motivated by time simulation issues. The emitted magnetic fields are below the limits imposed by ICNIRP or IEEE standards for a distance beyond of 7 cm. The impact of ferrite shielding is well reproduced by the proposed simulation model. A correlation between simulation and experimental results close to 2% demonstrates the accuracy of the adopted simulation approach for the driving electronic circuitry. Thus the proposed modeling and simulation approach can be an useful tool for an efficient design and optimization of an effective WPTS.

#### REFERENCES

- [1] Z. D. Chen, S. Kawasaki and N. B. Carvalho, "Wireless power transmission—The last cut of wires...", IEEE Microwave Magazine, vol. 14, n°2, pp. 22-24, March/April 2013.
- [2] B. W. Flynn and K. Fotopoulou, "Rectifying loose coils wireless power transfer in loosely coupled inductive links with lateral and angular misalignment," IEEE Microwave Magazine, pp. 48-54, March/April 2013.
- [3] I. Mayordomo, T. Dräger, P. Spies, J. Bernhard and A. Pflaum, "An overview of technical challenges and advances of inductive wireless power transmission," Proc. of the IEEE, vol. 101, no. 6, June 2013.
- [4] R. M. Dickinson, "Power in the sky requirements for microwave wireless power beamers for powering high-altitude platforms," IEEE Microwave Magazine, pp. 36-47, March/April 2013.
- [5] Z. Popovic, "Cut the cord low-power far-field wireless powering," IEEE Microwave Magazine, pp. 55-62, March/April 2013.
- [6] www.wirelesspowerconsortium.com
- [7] www.powermatters.org/
- [8] www.a4wp.org/
- [9] E. Waffenschmidt, "Wireless power for mobile devices," Philips Research Europe.
- [10] J. Muhlethaler, "Modeling and multi-objective optimization of inductive power components," Ph.D. dissertation, Swiss Federal Institute of Technology Zurich (ETHZ), 2012
- [11] U-M. Jow and M. Ghovanloo, "Design and optimization of printed spiral Coils for efficient transcutaneous inductive power transmission," IEEE Trans. on Biomedical Circuits and Systems, vol. 1, no. 3, Sep 2007.
- [12] S. C. Tang, S. Y. R Hui, and H. Chung, "Coreless planar printed-circuit-board (PCB) transformers – A fundamental concept for signal and energy transfer," IEEE Trans. Power Electron., vol. 15, no. 5, pp. 931-941, Sep. 2000.
- [13] "System description wireless power transfer," Version 1.1.1, Wireless Power Consortium, July 2012.
- [14] "ICNIRP Guidelines for limiting exposure to time-varying electric and magnetic fields (1 Hz – 100 kHz)," Health physics 99(6):818-836; 2010
- [15] "C95.1-2005 – IEEE standard for safety levels with respect to human exposure to radio frequency electromagnetic fields, 3 kHz to 300 GHz"